

Evidence of Slater-type mechanism as origin of insulating state in Sr_2IrO_4

Vijeta Singh^{1,2} and J. J. Pulikkotil^{1,2}

Academy of Scientific & Innovative Research (AcSIR), CSIR-NPL, New Delhi 110012
National Physical Laboratory, Council of Scientific & Industrial Research, New Delhi 110012

For iridates with large spatially extended $5d$ orbitals, it may be anticipated that distant neighbor interactions would play a crucial role in their ground state properties. From this perspective, we investigate the magnetic structure of Sr_2IrO_4 by including interactions beyond first and second neighbors, via supercell modeling. Adopting to first-principles scalar relativistic methods, it is found that the minimum in total energy among various magnetic structures correspond to a $\uparrow\uparrow\downarrow\downarrow$ type antiferromagnetic ordering of the Ir ions for which the magnitude of the electronic gap, that of the Ir local moments and, the facsimile of the two-peaked structure in the optical conductivity spectra of Sr_2IrO_4 were found to be in good agreement with the experiments. The results unequivocally evidence that the origin of the electronic gap in Sr_2IrO_4 is due to an unconventional antiferromagnetic ordering of Ir ions, thereby classifying the system as a Slater magnet, rather than the spin-orbit coupling driven $J_{eff} = \frac{1}{2}$ Mott insulator.

Sr_2IrO_4 is an insulator at all temperatures [1–9] and undergoes an antiferromagnetic transition below 240 K [6–10, 12–14]. Assuming that the strength of spin-orbit coupling (SOC) is comparable with that of crystal field interaction, Coulomb correlation and Hund’s coupling, a new quantum paradigm has been proposed [1]. In this model, the crystal field split Ir t_{2g} states are further split by SOC into a four-fold degenerate $J_{eff} = \frac{3}{2}$ quartet and a two-fold $J_{eff} = \frac{1}{2}$ doublet states. With Ir in its +4 formal valence state, the low energy $J_{eff} = \frac{3}{2}$ states are fully filled with two electrons each, leaving the $J_{eff} = \frac{1}{2}$ doublet singly occupied. Furthermore, since the bandwidth of the $J_{eff} = \frac{1}{2}$ doublets are significantly narrow, Coulomb correlation splits the doublets into an upper and lower Hubbard band, thereby rendering the system an insulating ground state [1, 15]. The model successfully accounts for both electron localization and insulating state on equal footing and derive consistent support from resistivity measurements, photo-emission spectroscopy, optical conductivity, absorption spectroscopy and model Hamiltonian based calculations [1, 2, 10, 11].

However, few observations had also hinted to itinerant characteristics in Sr_2IrO_4 [7, 16–19]. Scanning tunneling microscopy finds that the electronic gap emerges in the close vicinity of the magnetic transition [17], whereas optical conductivity measurement deduce a strong reduction in the optical gap with increasing temperature [41]. Also, a metal-insulator transition is observed in the ultrafast dynamics of photo-excited carriers which indicate to a underlying Slater-type mechanism in Sr_2IrO_4 [23]. Magnetic susceptibility and isothermal magnetization measurements find the effective paramagnetic moment and the saturation moment as $0.5 \mu_B$ and $0.14 \mu_B$, respectively which is far less than the expected spin-only value of $1 \mu_B$ for localized spin of $S = \frac{1}{2}$ [6, 7, 20]. The reduction in the magnitude of the Ir moment indicates to strong hybridization between Ir $5d$ and O $2p$ orbitals. In addition, Sr_2IrO_4 displays weak ferromagnetism which is attributed to spin canting [2, 12, 15, 20]. It has been addressed in terms of nontrivial exchange interactions ac-

counting for the strong coupling of orbital magnetization to the lattice [24, 25]. The weak ferromagnetism although vanishes with increasing pressure, system retains the insulating ground state [26]. The effect is attributed to an increased tetragonal crystal field thereby substantiating the interplay of structural distortions and SOC, which affects the balance between the isotropic magnetic coupling and the Dzyaloshinskii-Moriya anisotropic interaction. It is also highlighted that distorted in-plane bond angle in Sr_2IrO_4 can be tuned through magnetic field [27] and epitaxial strain [28]. Besides, the in-plane anisotropic nature and inter-layer coupling are also seen to play an important role in the low field magnetic nature of Sr_2IrO_4 [29]. Therefore, in the view of these experimental findings, it is clear that there is a subtle interplay of SOC, crystal field, Coulomb correlations, magnetic exchange interactions, and the local chemistry of the underlying IrO_6 motifs in Sr_2IrO_4 .

Significantly, what appears less emphasized in Sr_2IrO_4 is the effect of distant near neighbor interactions on the magnetism and its electronic structure properties. The magnetic structure as refined from neutron diffraction associates a non-collinear Neel type ordering of the Ir spins in the crystallographic $a - b$ plane, with the spin orientation rigidly tracking the staggered rotation of the IrO_6 along the c -axis [20]. However, the Ir $5d$ orbitals being much extended in space and that they strongly hybridize with the near neighboring O $2p$ orbitals, it may be anticipated that the magnetic interactions in the $a - b$ plane would significantly extend over distant neighbors than those along the c -axis. The antiferromagnetic ordering temperature as high as 240 K, can be well thought of one such consequence of distant neighbor magnetic exchange interactions.

Here, we present a comprehensive investigation of the electronic and magnetic structure of Sr_2IrO_4 , by means of first principles density functional theory. To include interactions beyond first nearest neighbors, we model few antiferromagnetic structures on an underlying super-cell of dimension $2a \times 2a \times c$, where a and c are the tetragonal lattice parameters of Sr_2IrO_4 . Consistent with the

previous works, we find that the local approximations to the exchange correlation potential, such as local density approximation (LDA) [21] and generalized gradient approximation (GGA-PBE) [22] fail to capture the antiferromagnetic insulating ground state of Sr_2IrO_4 . However, using the modified Becke-Johnson potential (mBJ) [31], we find that the equilibrium corresponds to an unconventional $\uparrow\uparrow\downarrow\downarrow$ type antiferromagnetic ordering of the Ir ions in the a - b plane. The predictive powers of the calculation are substantiated by the consistency it yields with the experiments. The magnitude of the insulating gap and that of the Ir local moment and, the double peak structure in the materials optical absorption spectra are found to be in good agreement with the experiments. These findings suggest that the underlying mechanism that drives Sr_2IrO_4 as an antiferromagnetic insulator is Slater-type, which is in stark contrast with the widely discussed SOC driven $J_{\text{eff}} = \frac{1}{2}$ Mott model.

Calculations are based on the full potential linearized augmented plane-wave (FP-LAPW) method as implemented in the Wien2k code [30]. The lattice parameters were adopted to the experimental values, with $a = 5.48$ Å, and $c = 25.83$ Å [12], and the position coordinates of the Sr and O ions were fully relaxed. The ground state properties were obtained using well-converged basis sets using the Wien2k parameters; $R_{\text{MT}}K_{\text{max}} = 7$, $G_{\text{max}} = 24$ a.u.⁻¹ and $l_{\text{max}} = 7$ [30]. Additional local orbitals were also used to account for the semi-core Ir $5p$ states. The exchange correlation potential to the crystal Hamiltonian was considered in mBJ formalism [31].

Few collinear magnetic structures with different initial Ir spin alignment were considered in the study. These are shown in Table I, which are described in terms of the Ir spin alignment in the first, second, third and fourth near neighbors designated as $d_{\text{NN}}^{(i)}$; $i = 1, 4$. Neglecting non-collinearity, AF1 then represents the experimentally determined structure and FM represents ferromagnetic ordering. In LDA spin polarized calculations, all structures converged to a paramagnetic metallic solution. However, in GGA the AF3 spin configuration converged to an antiferromagnetic metallic solution with an Ir moment of $0.2 \mu_B$, while all other structures converged to a nonmagnetic solution. The AF3 structure was -1.4 meV/f.u lower in energy in comparison to its non-magnetic counterpart. A schematic representation of the AF3 structure is shown in Fig.1. The AF3 unit cell consists of 16 formula units, with an underlying $Pnna$ symmetry of crystal lattice dimensions $a = 5.48$ Å, $b = 25.83$ Å and $c = 10.96$ Å.

It is well known that the electron density representation of the Coulomb potential in both LDA and GGA leads to an unphysical self interaction. As a result, these approximations tend to reduce the self-repulsion of electrons thereby stabilizing artificially delocalized electronic states [33, 34]. Among various correction schemes that have been proposed [35–37], we adopt to the mBJ formalism. With t and ρ representing the kinetic energy density and electron density, respectively, a screening term of

	Space group	$d_{\text{NN}}^{(1)}$ (3.88 Å)	$d_{\text{NN}}^{(2)}$ (5.48 Å)	$d_{\text{NN}}^{(3)}$ (7.01 Å)	$d_{\text{NN}}^{(4)}$ (7.75 Å)
AF1	$I-4_2d$	4(↓)	4(↑)	4(↑) 4(↓)	4(↑)
AF2	$P4_12_12$	2(↑) 2(↓)	4(↓)	4(↑) 4(↓)	4(↑)
AF3	$Pnna$	2(↑) 2(↓)	2(↑) 2(↓)	4(↑) 4(↓)	4(↓)
FM	$I4_1/acd$	4(↑)	4(↑)	8(↑)	4(↑)

Table I: : Table showing the spin ordering and the space group of the magnetic structures, generated using $2 \times 2 \times 1$ super-cell framework. Here, $d_{\text{NN}}^{(i)}$ represents the i^{th} near neighboring shell with respect to a central Ir spin (↑) ion. The first four near neighboring distances are also shown.

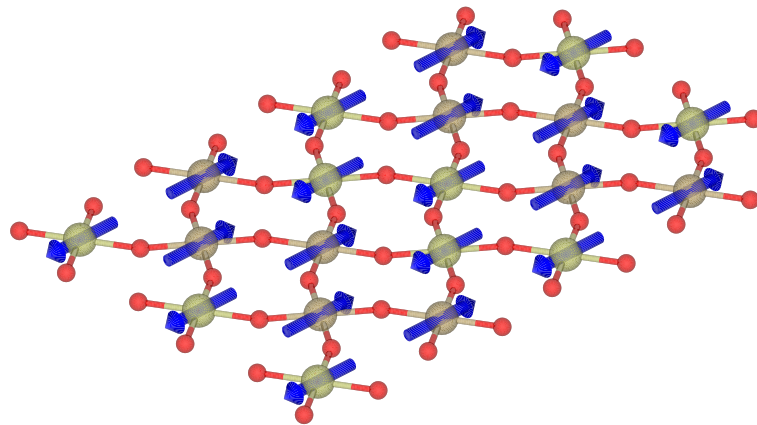


Figure 1: The schematic representation of the AF3 structure showing the antiferromagnetic ordering of Ir moments in the $a - b$ plane of Sr_2IrO_4 .

the form $\sqrt{\frac{t}{\rho}}$ is introduced in the mBJ exchange potential, the contribution of which is calculated by $\frac{|\nabla\rho|}{\rho}$ [31]. As a result, regions with low density are associated with higher positive potential thereby increasing the energy of these states [31, 38]. The mBJ formalism is applicable for Sr_2IrO_4 and also for other iridates [39, 40] since the states in the vicinity of Fermi energy are predominantly anti-bonding in character. It should be noted that the anti-bonding orbitals have less electron density, thus the choice of mBJ exchange potential for iridates is well justified.

In Fig.2, we show the mBJ generated total, atom resolved and Ir $5d$ resolved density of states (DOS) of Sr_2IrO_4 with AF3 spin configuration in the Ir sub-lattice. The spectra reveal Sr_2IrO_4 to be an insulator with an electronic gap of 0.47 eV, consistent with the experimental value of 0.54 eV [41]. Here, we note that the magnitude of the insulating gap in Sr_2IrO_4 have been reported

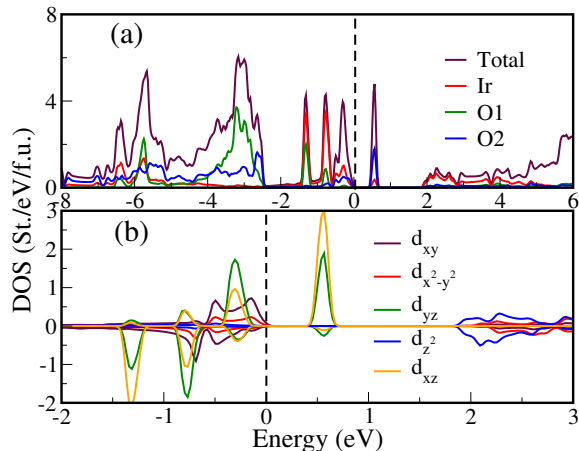


Figure 2: (color online): The mBJ density of states of the AF3 antiferromagnetic structure. (a) Total and atom resolved partial density of states for the AFM unit-cell and, (b) Ir 5d resolved partial density of states per Ir atom. Here, the O1 and O2 atoms represent the apical and in-plane O atoms, respectively. The broken line through energy zero represents the reference Fermi energy.

between 0.1–0.6 eV, with the lowest determined from the resistivity data fit using a thermal activation model [14, 27] and also from the earlier GGA+U+SOC calculations [1, 3]. The highest value of the insulating gap of 0.6 eV follows from the density of states measurements using the scanning tunneling spectroscopy [43]. Intermediate values of the gap are reported from the optical conductivity, resonant inelastic x-ray scattering [1, 3, 15] and also from the photoemission spectroscopy measurements [1, 44, 45].

In accordance with the ionic model which associates Ir 5d manifold with five electrons, the electronic gap is found to reside well within the Ir t_{2g} manifold which extends over the range $E(\text{eV}) \in [-1.5, 0.8]$. Four distinct localized features, which are predominantly of Ir d_{xz} / d_{yz} orbital characters are observed in the spectra. Three of them are in the occupied part of the spectra centered at -1.32 , -0.77 and -0.31 eV below E_F and, the fourth peak at 0.55 eV above E_F . The position of these bands indicate to three Ir t_{2g} inter-band transitions with the first, second and third transition energies being $\simeq 0.86$ eV, 1.32 eV and 1.87 eV, respectively. These energies are reasonably in good agreement with the optical conductivity measurements, where two transition peaks labeled α and β were determined to be at $\simeq 0.5$ eV and 1 eV, respectively [41, 42].

However, unlike the d_{xz} / d_{yz} states, the d_{xy} states appear relatively more widespread on the energy scale. We note that the Ir-O distance in Sr_2IrO_4 corresponds to 1.98 Å and 2.04 Å, for in-plane and apical O ions, respectively. For the in-plane O2 ions, the $2p_z$ orbitals hybridize with the Ir d_{xz} and d_{yz} orbitals, while the O $2p_x$ and $2p_y$ mix with the d_{xy} , d_{z^2} and $d_{x^2-y^2}$ orbitals. On the other hand, for apical O1 ions the $2p_z$ orbitals

hybridize with the Ir d_{z^2} and the $2p_x$ / $2p_y$ mix with the d_{xz} / d_{yz} states. Thus, the crystal chemistry suggests a mixing of the Ir t_{2g} and e_g states in Sr_2IrO_4 primarily due to the rotation of the IrO_6 octahedra. The rotation of the octahedra mixes the otherwise orthogonal Ir d_{xy} and $d_{x^2-y^2}$ orbitals and consequently push the d_{xy} states below the Fermi energy. The d_{xy} and $d_{x^2-y^2}$ hybridization also results in a pseudo-gap like feature which is manifested $\simeq -0.6$ eV below E_F . Further, the valence band energy integration of the orbitals states showed that the $d_{xy} + d_{x^2-y^2}$ orbitals are occupied with $\simeq 2$ electrons per Ir ion, while the electron occupation in the $d_{xz} + d_{yz} + d_{z^2}$ sums to 3 electrons per Ir ion, with d_{xz} and d_{yz} occupancy being 1.15 and 1.29 electrons, respectively. Also, the integrated DOS of the d_{xy} / d_{yz} orbitals above E_F was determined to be $\simeq 1$ e⁻ per Ir ion. Thus, we find that the scalar relativistic calculations with exchange potential as described in the mBJ formalism predicts Sr_2IrO_4 to be an antiferromagnetic insulator.

The magnitude of the local magnetic moment at the Ir sites in the AF3 structure was calculated as $\simeq 0.57 \mu_B$. The value is significantly higher than those determined from experiment, the latter which deduce the value as $0.2 \mu_B$ [20]. The overestimation of the Ir local moment might be due to the PBE-GGA functional in the calculation. However, the Ir magnetic moment is found to be much smaller than spin only value of $1 \mu_B$ anticipated for a $S = \frac{1}{2}$ system. This may be partly attributed to the strong hybridization of the Ir 5d – O 2p orbitals. The effects of hybridization are also manifested on the induced moments at the O sites. We note that the AF3 structure has a $\uparrow\uparrow\downarrow$ type antiferromagnetic ordering of Ir ions in the $a-b$ plane of the tetragonal unit cell. For those in-plane O ions which bridge the Ir ions in the $a-b$ plane with same polarization, *i.e.*, $\uparrow\uparrow$ or $\downarrow\downarrow$ the induced magnetic moment is calculated as $\simeq 0.12 \mu_B$ while for oppositely polarized Ir ions the moment is $\simeq 0.06 \mu_B$. The induced moments on the apical O ions were found to be $0.03 \mu_B$.

One of the well accepted methods to validate the electronic structure is by its optical response. In experiments, a double-peak structure with maxima around 0.5 eV and 1 eV have been observed, with the former peak being relatively sharper than the latter [15, 42, 47]. These peaks are associated with two Ir $d-d$ transitions, which in terms of the J_{eff} model are due to the transitions from occupied $J_{eff} = \frac{3}{2}$ and $\frac{1}{2}$ states to the unoccupied $J_{eff} = \frac{1}{2}$ states. The spectra has been well reproduced by the LDA+U+SO calculations, thereby suggesting the importance and interplay of SOC and Coulomb correlations in Sr_2IrO_4 [1].

In Fig. 3, we show the optical conductivity calculated for Sr_2IrO_4 with the underlying AF3 structure. Consistent with the experimental spectra, we obtain two characteristic peaks, centered on the energy scale at $\simeq 0.82$ eV and 1.32 eV, respectively. We note that the position of the peaks are shifted to higher energies in comparison with experiments [42, 46] which is primarily due to the larger band gap estimated (0.57 eV) in our calcu-

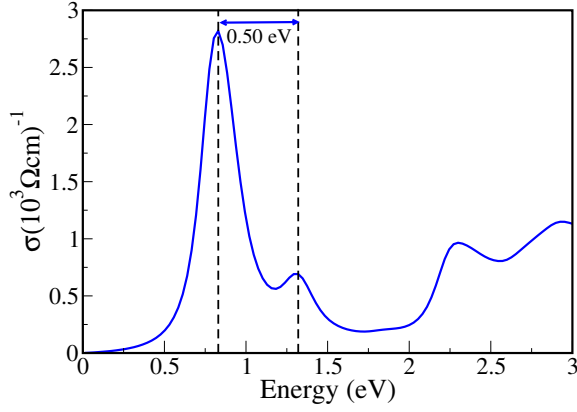


Figure 3: The calculated optical conductivity spectra of Sr_2IrO_4 using the scalar relativistic Hamiltonian with an underlying AF3 structure. Two peaks correspond to Ir $d-d$ transitions and are positioned at 0.82 eV and 1.32 eV, respectively. The energy difference between the peaks corresponds to a magnitude of 0.5 eV.

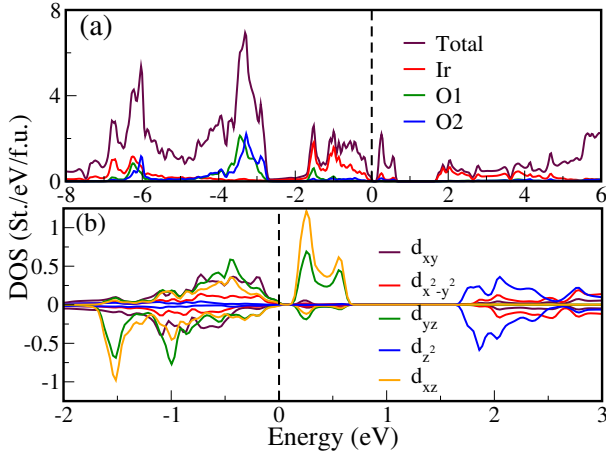


Figure 4: (color online): The mBJ-GGA+SOC density of states of the AF3 antiferromagnetic structure. (a) Total and atom resolved partial density of states for the AFM unit-cell and, (b) The Ir $5d$ resolved partial density of states. Here, the O1 and O2 atoms represent the apical and in-plane O atoms, respectively. The broken line through energy zero represents the reference Fermi energy.

lations. However, what is very consistent between the experiments and that of our results is the energy difference between the two peaks, which is found to be 0.5 eV. Our results, therefore show that the origin of electronic gap in Sr_2IrO_4 is associated with the long ranged antiferromagnetic interactions, and hence a Slater-insulator.

We also investigated the effect of spin-orbit coupling (SOC) on the electronic structure of Sr_2IrO_4 . The GGA-mBJ+SOC density of states are shown in Fig.4. In the calculation the SOC was included for the valence states

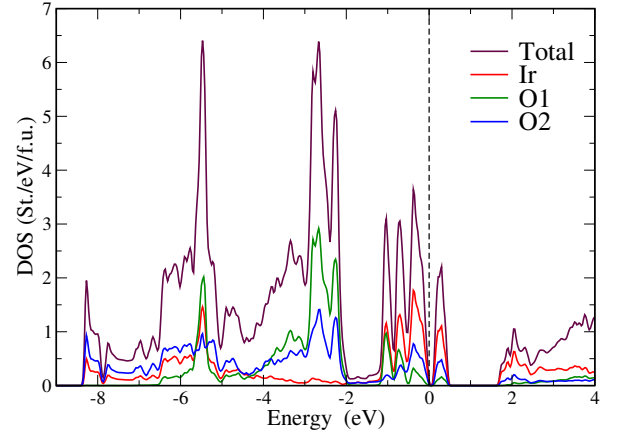


Figure 5: (color online): The density of states of the AF3 antiferromagnetic structure calculated in the GGA+ U_{eff} ($U_{eff} = 2$ eV) Hamiltonian, showing the total and atom resolved partial density of states. Here, the O1 and O2 atoms represent the apical and in-plane O atoms, respectively. The broken line through energy zero represents the reference Fermi energy.

through the second variational step with the mBJ scalar relativistic basis, where states up to 10 Ry above E_F were included in the basis expansion. While the overall features of bonding states are more or less unaltered, we find noticeable changes in the anti-bonding region. The Ir $5d$ bands are more broadened manifesting an enhanced hybridization of the t_{2g} states with the O $2p$ orbitals. The hybridization not only is found to reduce the band gap to 0.17 eV, but also decreases the magnitude of the Ir local magnetic moment to $0.47 \mu_B$.

So to check whether the insulating gap is originally due to the unconventional antiferromagnetic ordering of Ir spins and not pertained to the choice of the exchange functional, we also performed GGA+ U_{eff} calculations, with $U_{eff} = 2$ eV. Quite interestingly, the overall features in the density of states (Fig.5) were found very much similar to that obtained with the mBJ-GGA. However, the calculated band gap and Ir local moment was 0.11 eV and $0.41 \mu_B$, respectively. In general, our results following a comprehensive set of calculations concisely and convincingly show that SOC is lesser significant interaction in rendering Sr_2IrO_4 an antiferromagnetic insulating ground state.

In summary, using the first-principles density functional theory based scalar relativistic calculations with exchange potential described in mBJ formalism, we find that Sr_2IrO_4 is an unconventional Slater-type antiferromagnetic system. The calculated magnitude of the electronic gap, that of the Ir local moment and, the two peak structure in the materials optical conductivity are found to be very consistent with the experimental results. Contrary to the present understanding that Sr_2IrO_4 is a SOC driven J_{eff} Mott insulator, our calculations show that the role of SOC in Sr_2IrO_4 is of lesser significance in rendering the system its insulating ground state. Our

results, which are based on density functional theory, are expected to stimulate further experimental works with an objective to unravel the magnetic structure of the system

and the nature of Ir magnetism, thereby providing robust understanding of iridates, in general.

-
- [1] B. J. Kim, H. Jin, S. J. Moon, J.-Y. Kim, B.-G. Park, C. S. Leem, J. Yu, T. W. Noh, C. Kim, S.-J. Oh, J.-H. Park, V. Durairaj, G. Cao, and E. Rotenberg, *Phys. Rev. Lett.* 101, 076402 (2008).
 - [2] B. J. Kim, H. Ohsumi, T. Komesu, S. Sakai, T. Morita, H. Takagi, and T. Arima, *Science* 323, 1329 (2009).
 - [3] H. Jin, H. Jeong, T. Ozaki, and J. Yu, *Phys. Rev. B* 80, 075112 (2009).
 - [4] M. V. R. Rao, V. G. Sathe, D. Sornadurai, B. Panigrahi, and T. Shripathi, *J. Phys. Chem. Solids* 61, 1989 (2000).
 - [5] B. Fisher, J. Genossar, A. Knizhnik, L. Patlagan, and G. M. Reisner, *J. Appl. Phys.* 101, 123703 (2007).
 - [6] G. Cao, J. Bolivar, S. McCall, J. E. Crow, and R. P. Guertin, *Phys. Rev. B*, 57, R11039 (1998).
 - [7] N. S. Kini, A. M. Strydom, H. S. Jeevan, C. Geibel, and S. Ramakrishnan, *J. Phys. Condens. Matter* 18, 8205 (2006).
 - [8] C. Cosio-Castaneda, G. Tavizon, A. Baeza, P. de la Mora, and R. Escudero, *J. Phys. Condens. Matter* 19, 446210 (2007).
 - [9] Y. Klein and I. Terasaki, *J. Phys. Condens. Matter* 20, 295201 (2008).
 - [10] S. Chikara, O. Korneta, W. P. Crummett, L. E. DeLong, P. Schlottmann, and G. Cao, *Phys. Rev. B* 80, 140407 (2009).
 - [11] T. Takayama, A. Matsumoto, G. Jackeli and H. Takagi, *Phys. Rev. B* 94, 224420 (2016)
 - [12] M. K. Crawford, M. A. Subramanian, R. L. Harlow, J. A. Fernandez-Baca, Z. R. Wang, and D. C. Johnston, *Phys. Rev. B* 49, 9198 (1994).
 - [13] R. J. Cava, B. Batlogg, K. Kiyono, H. Takagi, J. J. Krajewski, W. F. Peck, L. W. Rupp, and C. H. Chen, *Phys. Rev. B* 49, 11890 (1994).
 - [14] T. Shimura, Y. Inaguma, T. Nakamura, M. Itoh, and Y. Morii, *Phys. Rev. B* 52, 9143 (1995).
 - [15] J. Kim, D. Casa, M. H. Upton, T. Gog, Y. J. Kim, J. F. Mitchell, M. van Veenendaal, M. Daghofer, J. van den Brink, G. Khaliullin and B. J. Kim, *Phys. Rev. Lett.* 108, 177003 (2012).
 - [16] R. Arita, J. Kuneš, A. V. Kozhevnikov, A. G. Eguiluz, and M. Imada, *Phys. Rev. Lett.* 108, 086403 (2012).
 - [17] Q. Li, G. Cao, S. Okamoto, J. Yi, W. Lin, B. Sales, J. Yan, R. Arita, J. Kuneš, A. Kozhevnikov, A. Eguiluz, M. Imada, Z. Gai, M. Pan, and D. Mandrus, *Sci. Rep.* 3, 3073 (2013).
 - [18] A. Yamasaki, H. Fujiwara, A. Higashiya, A. Irizawa, O. Kirilmaz, F. Pfaff, P. Scheiderer, J. Gabel, M. Sing, T. Muro, M. Yabashi, K. Tamasaku, H. Sato, H. Namatame, M. Taniguchi, A. Hloskovskyy, H. Yoshida, H. Okabe, M. Isobe, J. Akimitsu, W. Drube, R. Claessen, T. Ishikawa, S. Imada, A. Sekiyama, and S. Suga, *Phys. Rev. B* 89, 121111(R) (2014).
 - [19] C. Piovera, V. Brouet, E. Papalazarou, M. Caputo, M. Marsi, A. Taleb-Ibrahimi, B. J. Kim, and L. Perfetti, *Phys. Rev. B* 93, 241114(R) (2016).
 - [20] F. Ye, S. Chi, B. C. Chakoumakos, J. A. Fernandez-Baca, T. Qi and G. Cao, *Phys. Rev. B* 87, 140406 (2013).
 - [21] J. P. Perdew and Y. Wang *Phys. Rev. B* 45, 13244 (1992).
 - [22] J. P. Perdew, K. Burke, and M. Ernzerhof *Phys. Rev. Lett.* 77, 3865 (1996)
 - [23] D. Hsieh, F. Mahmood, D. H. Torchinsky, G. Cao, and N. Gedik *Phys. Rev. B* 86, 035128 (2012).
 - [24] G. Jackeli and G. Khaliullin, *Phys. Rev. Lett.* 102, 017205 (2009).
 - [25] P. Liu, S. Khmelevskiy, B. Kim, M. Marsman, D. Li, X.-Q. Chen, D. D. Sarma, G. Kresse, and C. Franchini, *Phys. Rev. B* 92, 054428 (2015).
 - [26] D. Haskel, G. Fabbri, M. Zhernenkov, P. P. Kong, C. Q. Jin, G. Cao, and M. van Veenendaal, *Phys. Rev. Lett.* 109, 027204 (2012).
 - [27] M. Ge, T. Qi, O. Korneta, D. DeLong, P. Schlottmann, W. Crummett, and G. Cao, *Phys. Rev. B* 84, 100402 (2011).
 - [28] C. R. Serrao, J. Liu, J. T. Heron, G. Singh-Bhalla, A. Yadav, S. J. Suresha, R. J. Paull, D. Yi, J. H. Chu, M. Trassin, A. Vishwanath, E. Arenholz, C. Frontera, J. Zelezny, T. Jungwirth, X. Marti and R. Ramesh, *Phys. Rev. B* 87, 085121 (2013).
 - [29] Y. Gim, A. Sethi, Q. Zhao, J. F. Mitchell, G. Cao and S. L. Cooper, *Phys. Rev. B* 93, 024405 (2016).
 - [30] P. Blaha, K. Schwarz, G. Madsen, D. Kvasnicka, and J. Luitz, computer code WIEN2K, Technical University of Vienna, Vienna (2001).
 - [31] F. Tran and P. Blaha, *Phys. Rev. Lett.* 102, 226401 (2009).
 - [32] V. Singh and J. J. Pulikkotil, *Phys. Chem. Chem. Phys.*, 18, 26300 (2016).
 - [33] A. J. Cohen, P. Mori-Sanchez, and W. Yang, *Science* 321, 792 (2008).
 - [34] P. Mori-Sanchez, A. J. Cohen, and W. Yang, *Phys. Rev. Lett.* 100, 146401 (2008).
 - [35] J. Heyd, J. E. Peralta, G. E. Scuseria, and R. L. Martin, *J. Chem. Phys.* 123, 174101 (2005).
 - [36] F. Bechstedt, F. Fuchs, and G. Kresse, *Phys. Status Solidi B* 246, 1877 (2009).
 - [37] A. Georges, G. Kotliar, W. Krauth, and M. J. Rozenberg, *Rev. Mod. Phys.* 68, 13 (1996).
 - [38] D. Koller, F. Tran, and P. Blaha, *Phys. Rev. B* 83, 195134 (2011).
 - [39] V. Singh and J. J. Pulikkotil, *Phys. Chem. Chem. Phys.* 18, 26300 (2016).
 - [40] V. Singh and J. J. Pulikkotil, *Comput. Mater. Sci.* 153, 97-102 (2018).
 - [41] S. J. Moon, Hosub Jin, W. S. Choi, J. S. Lee, S. S. A. Seo, J. Yu, G. Cao, T. W. Noh, and Y. S. Lee *Phys. Rev. B* 80, 195110 (2009).
 - [42] C. H. Sohn, M.-C. Lee, H. J. Park, K. J. Noh, H. K. Yoo, S. J. Moon, K. W. Kim, T. F. Qi, G. Cao, D.-Y. Cho, and T. W. Noh, *Phys. Rev. B* 90, 041105(R) (2014).
 - [43] J. Dai, E. Calleja, G. Cao and K. McElroy, *Phys. Rev. B* 90, 041102 (2014).
 - [44] Q. Wang, Y. Cao, J. A. Waugh, S. R. Park, T. F. Qi, O.

- B. Korneta, G. Cao, and D. S. Dessau, Phys. Rev. B 87, 245109 (2013).
- [45] B. M. Wojek, M. H. Berntsen, S. Boseggia, A. T. Boothroyd, D. Prabhakaran, D. F. McMorrow, H. M. Rønnow, J. Chang, and O. Tjernberg, J. Phys. Condens. Matter 24, 415602 (2012).
- [46] D. Pröpper, A. N. Yaresko, M. Höppner, Y. Matiks, Y. L. Mathis, T. Takayama, A. Matsumoto, H. Takagi, B. Keimer, and A. V. Boris, Phys. Rev. B 94, 035158 (2016).
- [47] J. S. Lee, Y. Krockenberger, K. S. Takahashi, M. Kawasaki, and Y. Tokura, Phys. Rev. B, 85, 035101 (2012).